

# PrefixKV: Adaptive Prefix KV Cache is What Vision Instruction-Following Models Need for Efficient Generation

Ao Wang<sup>1</sup> Hui Chen<sup>2</sup> Jiaxin Li<sup>1</sup> Jianchao Tan<sup>4</sup> Kefeng Zhang<sup>4</sup> Xunliang Cai<sup>4</sup>  
 Zijia Lin<sup>1</sup> Jungong Han<sup>3</sup> Guiguang Ding<sup>1</sup>

<sup>1</sup>School of Software, Tsinghua University <sup>2</sup>BNRist, Tsinghua University

<sup>3</sup>Department of Automation, Tsinghua University <sup>4</sup>Meituan Inc.

## Abstract

Recently, large vision-language models (LVLMs) have rapidly gained popularity for their strong generation and reasoning capabilities given diverse multimodal inputs. However, these models incur significant computational and memory overhead during inference, which greatly hinders the efficient deployment in practical scenarios. The extensive key-value (KV) cache, necessitated by the lengthy input and output sequences, notably contributes to the high inference cost. Based on this, recent works have investigated ways to reduce the KV cache size for higher efficiency. Although effective, they generally overlook the distinct importance distributions of KV vectors across layers and maintain the same cache size for each layer during the next token prediction. This results in the significant contextual information loss for certain layers, leading to notable performance decline. To address this, we present PrefixKV. It reframes the challenge of determining KV cache sizes for all layers into the task of searching for the optimal global prefix configuration. With an adaptive layer-wise KV retention recipe based on binary search, the maximum contextual information can thus be preserved in each layer, facilitating the generation. Extensive experiments demonstrate that our method achieves the state-of-the-art performance compared with others. It exhibits superior inference efficiency and generation quality trade-offs, showing promising potential for practical applications. Code is available at <https://github.com/THU-MIG/PrefixKV>.

## 1. Introduction

Recent years have witnessed the significant advancements of large vision-language models (LVLMs) [2, 11, 15, 26, 36, 37, 72]. Based on the powerful Large Language Models (LLMs) [1, 3, 18, 28, 46, 50, 51, 63], these models integrate visual inputs, showing strong generation and reasoning abilities for various multimodal tasks. They demonstrate inspiri-

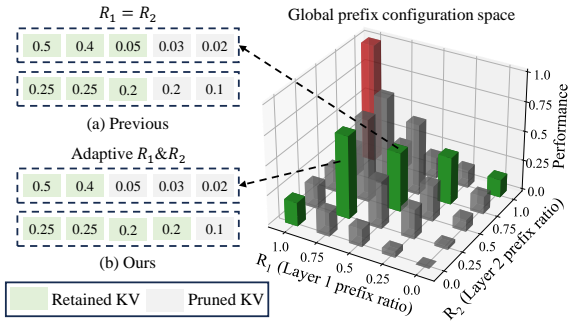


Figure 1. Comparison between previous methods and ours. Previous methods simply keep the same prefix length for priority sequences of KV, *i.e.*, retraining the same cache size for each layer. This causes notable information loss for certain layers. In this example, the first layer loses 30% of information. In contrast, we derive the optimal global prefix configuration to preserve as much information as possible in each layer. In this example, both layers can retain 90% of information, thereby enhancing performance.

ing application potential in various fields like autonomous driving [14, 57] and intelligent medical analyses [29, 52].

However, despite their remarkable capabilities, the efficient deployment of LVLMs encounters notable challenges in real-world scenarios. This stems from the typical Transformer architecture employed in the LVLMs, which necessitates the global interaction of tokens. During autoregressive decoding, the key and value vectors of previous tokens are thus required to be stored as the KV cache and subsequently retrieved by the output token [42]. The KV cache grows linearly with the number of processed tokens, which leads to notable memory overhead and heavy burden on GPU communication under lengthy sequences. This causes suboptimal efficiency, resulting in the inference bottleneck.

Given this, recent works have investigated pruning unimportant KV vectors or merging adjacent vectors to reduce the KV cache size while preserving the model performance [39, 61, 75]. For example, H<sub>2</sub>O [75] discards less important ones based on the attention scores. Elastic Cache [39] identifies the important KV vectors as the

anchor points and merges the surrounding less important cache with these anchors. While effective, existing works typically apply a uniform strategy that retains the same number of KV vectors for each layer to generate the next token efficiently, overlooking the layer-wise heterogeneous characteristics. Our analyses in Section 3.2 reveal the notably distinct importance distributions of KV vectors across layers, highlighting the need for tailored retention recipe for each layer. Intuitively, the importance distribution is concentrated in certain layers while relatively dispersed in other layers. As a suboptimal solution, retaining the same cache size for each layer during the next token prediction results in obvious information loss in dispersed layers, and redundant cache in concentrated layers, as shown in Figure 1.(a).

To address this, we present PrefixKV, a new KV cache compression method for efficient and accurate model generation. We define the prefix<sup>1</sup> of KV cache as the top ones in the priority sequences that are sorted KV vectors according to the normalized importance. The prefix KV vectors of each layer represents the retained cache, making the challenge of determining the optimal layer-wise cache size for the next token generation equivalent to identifying the optimal global prefix configuration. To derive such configuration for a given compression ratio budget, we leverage the prefix cumulative priority as the measurement for the amount of reserved contextual information in each layer. Binary search is then utilized to obtain the desirable information retention ratio, enabling the layer-wise KV retention aligns with the overall budget and maintains the ideal cumulative priority. This ensures that each layer can preserve maximal contextual information after compression, keeping the high generation quality of models, as shown in Figure 1.(b). Extensive experiments show that our method achieves the state-of-the-art performance compared with existing works. It can greatly boost the inference efficiency while well maintaining the model’s strong capabilities, exhibiting promising potential for real-world applications. Notably, with the compression budget of 20%, it provides  $1.8\times$  inference speedup for LLaVA-1.5-7B, attaining the competitive performance compared with original model.

## 2. Related Work

### 2.1. Vision instruction-following model

The progress of large vision-language models (LVLMs) has significantly expanded the capabilities of large language models (LLMs) [1, 2, 18, 28, 46–48, 50, 51] by incorporating visual information, leading to powerful generation and reasoning ability for multimodal tasks [4, 8–10, 15, 31, 36, 37, 79]. These models typically use linear projection [37] or perceivers [27] to integrate visual representations into the input of LLMs directly. Then, they are fur-

ther finetuned on high-quality instructional datasets, which include the image-text pairs and the language instructional commands. These models can thus follow multimodal instructions effectively and accurately. Inspired by the notable advancements, subsequent works have sought to enhance their region-level grounding ability [6, 11, 41, 72], 3D world perception [12, 23, 32, 64], semantic understanding [16, 53, 70, 74], and video comprehension [30, 33, 62, 71], etc. Other works also explore the applications of LVLMs in various practical scenarios, including industrial anomaly recognition [7, 22, 65], biomedical image understanding [29, 52], and autonomous driving and map systems [14, 49, 67], etc.

### 2.2. KV cache compression

While powerful, existing LVLMs typically encounter high inference costs due to the large parameter count and complex computation, which hinder their deployment for practical applications significantly. Like research on efficient vision models [24, 54–56, 59], numerous efforts have focused on improving the inference efficiency for LVLMs, including architectural design [13, 69, 77, 80], quantization [35, 38, 60], distillation [21, 25, 43], and pruning [40, 44, 45], etc. These methods typically focus on the compression on the model level, reducing the inference overhead brought by the parameters. Meanwhile, the KV cache on the data level also incurs significant memory usage and GPU communication overhead during inference. To address this, recent works have investigated various ways to compress the KV cache. For example, StreamingLLM [61] leverages the distance to the output token as the importance indicator and preserves the starting KV vectors and those adjacent to the output token. H<sub>2</sub>O [75] utilizes the attention scores as the importance metric for KV vectors and retains the important ones during generation. Elastic Cache [39] divides the KV cache into several buckets according to the positions of important KV cache and merges the vectors in the same bucket into one. Despite effective, they often overlook the distinct importance distribution across layers and simply retain the same KV cache size in each layer. This causes the notable information loss and significantly affects the model’s generation capability.

## 3. Methodology

In Section 3.1, we first introduce the basic inference process of LVLMs and the general KV cache compression framework. Then, in Section 3.2, we formalize the process of KV compression as retaining the prefix of KV cache and uncover the fact of diverse importance distributions of KV vectors in layers. This variation causes the obvious contextual information loss in existing methods. To address this, we present PrefixKV in Section 3.3, to deliver the ideal layer-wise cache size for the next token prediction by binary searching for the optimal global prefix configuration.

<sup>1</sup>Prefix refers to top elements sorted by importance instead of position.

### 3.1. Preliminary

LVLMs exhibit exceptional capabilities for multimodal instructions. Given an input which often consists of the system prompt and user instruction, they first embed the text into the token embeddings through the pre-defined vocabulary and transform the image as flattened patches through the visual encoder. Then, the model enters the prefilling stage, where all tokens interact with each other through the self-attention mechanism. Meanwhile, the key and value vectors of each token are stored as the KV cache, which keeps the contextual information for generation. Subsequently, the model transitions to the decoding stage and outputs the response in an autoregressive way. In each step, the latest predicted token serves as the input and it interacts with the cached KV vectors for preceding information by the self-attention module. It is worth noting that the KV cache size is proportional to the length of processed tokens. This can consume notable memory resources and result in bottleneck in inference speed. It calls for KV cache compression methods to reduce the KV cache size effectively.

The general KV cache compression framework in existing works consist of two stages [39, 61, 75]<sup>2</sup>. Firstly, after prefilling, the importance of each KV vector is derived based on the attention scores or the distance to the generated output. Then, the most important ones are retained in the cache while the less important KV vectors are removed to reduce the memory footprint. Meanwhile, the reserved KV cache sizes in layers meet the requirement of the compression ratio budget. Secondly, during the decoding stage, with the inclusion of KV vectors in the cache for newly generated tokens, the importance metric of each KV vector is updated. Less critical ones are removed to ensure that the cache size consistently aligns with the overall budget. Our method also follows this general framework, as shown in Figure 3. Specifically, after the prefilling, we retain the most important KV vectors by the ideal global prefix configuration. In the decoding, we follow [39] to prune the vectors at a fixed distance to the latest generated token and maintain the global prefix configuration to meet the target budget.

### 3.2. Layer-wise KV Cache Importance Distribution

**Mathematical notations for KV compression.** We first introduce the necessary notations to formalize the compression procedure. Specifically, we follow [39, 75] to employ the attention scores as the importance metric, which indicates the amount of contextual information of each KV vector. We suppose that the model consists of  $L$  transformer layers. For the  $l$ -th, layer, its input tokens  $\{t_l^1, t_l^2, \dots, t_l^N\}$  interact with each other in the multi-head self-attention module, where  $N$  is the token number. For the  $i$ -th head, we denote the query, key, and value vectors of the token  $t_l^n$

<sup>2</sup>For more preliminary, please refer to previous works [42, 66, 76, 78].

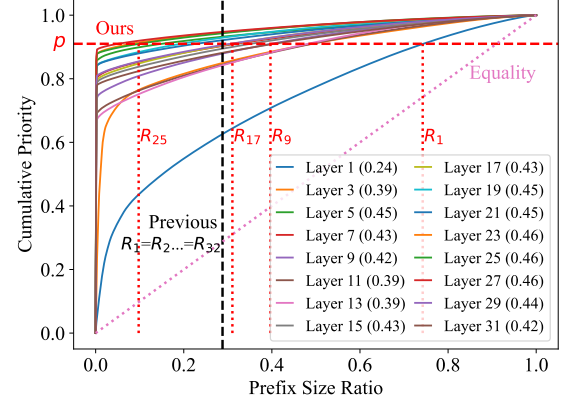


Figure 2. The lorenz curve of priority sequence for KV vectors in different layers. We observe that different layers exhibit diverse importance distributions in the KV cache. Previous methods (the dashed black line) that keep the same prefix cause the notable information loss in layers with dispersed distributions. In contrast, our method (the dashed red line) maximally retains the amount of contextual information of each layer by adaptively maintaining the maximal prefix cumulative priority. The numbers in parentheses in the legend represent the gini coefficient of priority sequence in each layer. A higher gini index indicates a more concentrated importance distribution. It quantitatively demonstrates the varying importance distributions of KV vectors across layers.

as  $q_l^{i,n}$ ,  $k_l^{i,n}$ , and  $v_l^{i,n}$ , respectively. Then, the causal attention score matrix  $A_l^i = \{a_l^{i,m,n}\}_{N \times N}$  can be derived by

$$a_l^{i,m,n} = \frac{\exp(q_l^{i,m} \cdot k_l^{i,n})}{\sum_{j \leq m} \exp(q_l^{i,m} \cdot k_l^{i,j})}, \quad (1)$$

where  $a_l^{i,m,n}$  indicates the attention score of token  $t_l^m$  with respect to token  $t_l^n$  in the  $i$ -th head. Then, the total attention score that each token  $t_l^n$  receives in the  $i$ -th head can be derived by  $\sum_m a_l^{i,m,n}$ . For each  $k_l^{i,n}$  and  $v_l^{i,n}$ , we follow [39] to define their importance metric as the averaged total attention score of  $t_l^n$  across all heads, *i.e.*,

$$I_l^n = \text{Average}_i(\sum_m a_l^{i,m,n}), \quad (2)$$

where  $\text{Average}_i$  denotes the average operation for heads. It is noted that the importance metric of each KV vector varies at each layer but is the same across heads. Then, for a compression ratio budget  $r$ , the top  $R_l$  proportion of KV vectors with the highest importance are retained in each head at the  $l$ -th layer. Besides, the adoption of  $\{R_1, R_2, \dots, R_L\}$  satisfy the requirement of  $\sum_{l=1}^L R_l N = rLN$ .

**Distinct importance distributions across layers.** Existing KV cache compression methods usually retain the same number of KV vectors for each layer. This, however, overlooks the diverse contextual information distribution across layers and causes notable valuable information loss.

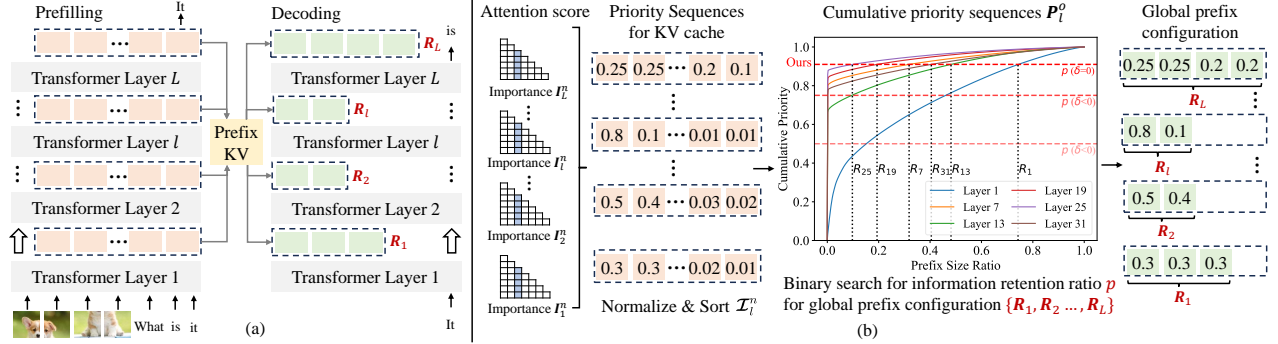


Figure 3. (a) The inference process of LVLMs, where the orange and green rectangles denote the KV cache generated during prefilling and utilized during decoding, respectively. After prefilling, the KV cache is layer-wisely compressed according to the proportions specified by PrefixKV, *i.e.*,  $\{R_1, \dots, R_L\}$ . During decoding, as the sequence lengthens and cache increases, the KV cache consistently maintains the derived compression proportions by pruning KV at a fixed distance [39]. (b) The overview of PrefixKV. It employs binary search for cumulative priority sequences of KV to derive the optimal global prefix configuration, which delivers ideal cache size ratio for each layer.

To uncover this fact, we leverage the lorenz curve [19, 20] to characterize the importance distribution across different layers. Specifically, for the  $n$ -th KV vector of  $l$ -th layer, we first obtain its importance ratio relative to all tokens by normalization, *i.e.*,  $\mathcal{I}_l^n = \frac{I_l^n}{\sum_{j=1}^N I_l^j}$ . We then sort the importance set  $\{\mathcal{I}_l^1, \mathcal{I}_l^2, \dots, \mathcal{I}_l^N\}$  in the descending order to derive the priority sequence of KV vectors. In the priority sequence, the vectors ranked higher have larger importance, making the KV compression equivalent to retaining the prefix of KV cache. Suppose that the sorted indices are  $\{s_l^1, s_l^2, \dots, s_l^N\}$ , for each prefix size ratio  $o$  of this sequence, we can obtain its cumulative priority by

$$P_l^o = \sum_{j \leq oN} \mathcal{I}_l^{s_l^j}. \quad (3)$$

$P_l^o$  indicates the amount of contextual information kept in the  $l$ -th layer after retaining top  $o$  proportion of the most important KV vectors. By deriving the prefix size ratio sequence  $\{\frac{1}{N}, \frac{2}{N}, \dots, 1\}$  and its corresponding cumulative priority sequence  $\{P_l^{\frac{1}{N}}, P_l^{\frac{2}{N}}, \dots, P_l^1\}$ , we can then obtain the lorenz curve of the importance distribution. As shown in Figure 2, we observe that the cumulative priority growth trends vary significantly across layers. Previous works generally retain the same layer-wise cache size, *i.e.*, adopting the same prefix size ratio of KV cache with  $R_j = r, \forall j \in [1, L]$ . In this scenario, as shown in the dashed black line, different layers exhibit the markedly distinct cumulative priorities, *i.e.*,  $P_l^{R_j}$ . This suggests an uneven retention of contextual information across layers, where layers showing rapid growth trends retain a substantial amount, whereas those with slower growth trends retain relatively little. This disparity leads to the obvious information loss in layers with slow growth and adversely impacts the generation quality. We also quantitatively show the diverse importance distribution by the gini coefficient [17, 20]. It is defined as the

area that lies between the equality line (the dotted pink line in Figure 2) and the lorenz curve. The smaller it is, the more uniform the importance distribution, and vice versa. As shown in the legend in Figure 2, different layers exhibit varying gini coefficients, further demonstrating the heterogeneity of KV cache in layers. This calls for adaptively determining the prefix of KV cache for each layer.

### 3.3. PrefixKV

Based on the above observations, we introduce PrefixKV. With layer-wise cache size scheme formalized as the global prefix configuration, it employs binary search to derive the ideal solution, as shown in Figure 3.(b).

**Global prefix configuration.** All layers' cache size ratios  $\{R_1, \dots, R_L\}$ , *i.e.*, the prefix size ratios of KV cache, constitute the global prefix configuration space of the model. The goal is to identify the optimal global prefix configuration to maintain the high quality of model generation. Given the compression ratio budget  $r$ , we discover a information retention ratio  $p$  to derive such configuration. Specifically, with the priority sequences,  $p$  represents the cumulative priority threshold. For the  $l$ -th layer, its proportion of retained KV vectors is thus the minimum prefix size ratio  $o$  such that the cumulative priority  $P_l^o$  in Equation (3) is larger than or equal to  $p$ , *i.e.*,  $R_l = \min\{o | P_l^o \geq p\}$ . Meanwhile, the value of  $p$  satisfies the requirement of the compression ratio budget, *i.e.*,

$$\sum_l R_l = \sum_l \min\{o | P_l^o \geq p\} = rL. \quad (4)$$

The corresponding prefix configurations  $\{R_1, \dots, R_L\}$  ensure that maximal prefix cumulative priority is kept layer-wisely. Finding  $p$  is needed for global prefix configuration.

**Binary search for optimal configuration.** Due to the numerous possible values of  $p$ , obtaining  $p$  is quite challenging. We propose employing binary search to efficiently

---

**Algorithm 1:** Binary Search for retention ratio  $p$ 

---

```
1 Initialize  $p_1 \leftarrow 0, p_2 \leftarrow 1$ ;  
2 while  $p_1 < p_2$  do  
3    $p \leftarrow \frac{p_1+p_2}{2}, \sum_l \mathbf{R}_l = \sum_l \min(\{o | \mathbf{P}_l^o \geq p\})$ ;  
4    $\delta = \sum_l \mathbf{R}_l - rL$ ;  
5   if  $\delta == 0$  then return  $p$ ;  
6   else if  $\delta < 0$  then  $p_1 \leftarrow p$ ;  
7   else  $p_2 \leftarrow p$ ;  
8 return  $p$ ;
```

---

derive  $p$  for adaptive layer-wise KV retention. Formally, we start with the interval of  $[p_1, p_2]$  where  $p_1 = 0$  and  $p_2 = 1$ . We try  $p = \frac{p_1+p_2}{2} = 0.5$  and calculate its corresponding compression budget difference  $\delta = \sum_l \mathbf{R}_l - rL$ . If  $\delta$  is equal to zero, we have found the value for  $p$ . If it is smaller than zero, we set  $p_1 = p$ ; otherwise, we set  $p_2 = p$ . Then, we update  $p = \frac{p_1+p_2}{2}$  and repeat the process until meeting the constraint. Algorithm 1 presents the process. In this way, as shown in the dashed red line in Figure 2, different layers can consistently keep the maximal amount of the contextual information. It ensures that the valuable KV vectors are cached and accessible during generation across all layers. The quality of the model’s outputs can be maintained even after significant compression of the KV cache. In practice,  $p$  that satisfies  $\delta = 0$  may not exist. We can thus set a small threshold for  $\delta$  to terminate the search and scale the resulting global prefix configuration to meet the budget.

Moreover, we observe that the cumulative priority sequences of layers are similar and robust across different samples. Therefore, given a compression ratio budget, we can leverage random samples to derive the corresponding  $p$  value and the optimal global prefix configuration  $\{\mathbf{R}_1, \mathbf{R}_2, \dots, \mathbf{R}_L\}$  for each layer offline, as analyzed in Figure 4, Table 5, and Table 6. The configuration can thus be adopted for the model during inference, which avoids the online binary search and shows good generalizability.

## 4. Experiments

### 4.1. Experimental Settings

We follow [39] to employ LLaVA-1.5-7B [36] and LLaVA-1.5-13B [36], and leverage the LLaVA-Description [39] and MM-Vet [68] instruction-following datasets for evaluation. LLaVA-Description is a curated subset of 1000 detailed description instructions from the LLaVA-1.5 training set [39]. MM-Vet encompasses a diverse set of tasks designed to comprehensively evaluate the model performance in both understanding and generation. Besides, we also re-conduct the instruction tuning for LLaVA-1.5 models, to exclude the LLaVA-Description for preventing data leakage during evaluation. We follow [39] to employ the perplexity (PPL) and the ROUGE score [34] metrics. Specifically, PPL quan-

tifies the exponential value of the cross-entropy loss between the predicted next token and ground truth. A lower PPL indicates the better generation quality. The ROUGE score calculates the longest common subsequence between the generated output and the reference outputs, with F1 score used for evaluation. A higher ROUGE score indicates the better consistency with reference responses.

Following [39], we utilize the model without cache compression to generate the reference output for the ROUGE score evaluation. Besides, in practice, multiple generation texts of a model can be different when the temperature is not zero. Thus, for the compression budget of 100%, *i.e.*, without compression, we measure the ROUGE score of two generation outputs and it is thus smaller than 1. For other budgets, we use the temperature of 0 for the reproducibility and the ROUGE score may thus exceed the uncompressed one. We simply leverage 10 random samples from the training set of model for the global prefix configuration estimation offline. During decoding, we follow [39] to fix the distance to the latest token for pruning and maintain the layer-wise cache size ratios to satisfy the target budget. We compare with the state-of-the-art Elastic Cache [39], Heavy-Hitter Oracle [75], and StreamingLLM [61], which are termed as Elastic, H<sub>2</sub>O, and Local for brevity, respectively.

### 4.2. Main Results

As shown in Table 1 and Table 2, our method consistently achieves the state-of-the-art performance compared with others across various compression budgets and different model scales. For example, as shown in Table 1, under a compression budget of 50% on LLaVA-Description, our PrefixKV significantly outperforms H<sub>2</sub>O and Elastic cache by 9.49 and 2.90 in PPL for LLaVA-1.5-7B. It also surpasses the Local cache by a notable margin of 0.39 in ROUGE score. We also observe that our advantages over others can be further amplified as the compression budget decreases. Under a compression budget of 20%, our PrefixKV can still maintain a satisfactory PPL of 3.69, which is reduced by 101.3, 44.6, and 10.3 compared with Local, H<sub>2</sub>O, and Elastic, respectively. For large model of LLaVA-1.5-13B, our method also demonstrates the notable superiority over others. For example, as shown in Table 2, our PrefixKV outperforms Elastic and H<sub>2</sub>O cache by 1.53 and 5.82 PPL, respectively, under a compression budget of 40% on MM-Vet. Furthermore, our method shows the minimal performance decline compared with the original model without KV compression in various scenarios. For example, as shown in Table 2, for LLaVA-1.5-13B, our method can maintain the nearly identical PPL and ROUGE scores compared with the uncompressed model at any compression budget exceeding 30%. Under a compression budget of 20%, our PrefixKV only leads to the decline of 0.44 PPL. These results well demonstrate the superiority of ours.

Table 1. Comparison with SOTA methods on LLaVA-Description with the PPL / ROUGE metrics under various compression ratio budgets. Note that a lower PPL is better, while a higher ROUGE is better. The results without the KV compression are 3.20 / 0.62 for LLaVA-1.5-7B and 2.73 / 0.63 for LLaVA-1.5-13B, respectively. It can be observed that our method consistently achieves superior performance.

Model	Method	10%	20%	30%	40%	50%	60%	70%	80%	90%
7B	Local	66.0 / 0.22	105 / 0.14	70.0 / 0.18	47.5 / 0.17	33.8 / 0.19	14.7 / 0.30	5.50 / 0.41	4.78 / 0.50	4.03 / 0.55
	H <sub>2</sub> O	54.5 / 0.28	48.3 / 0.31	32.0 / 0.33	18.3 / 0.32	12.9 / 0.34	7.50 / 0.41	4.28 / 0.51	4.16 / 0.53	3.72 / 0.57
	Elastic	18.0 / 0.29	14.0 / 0.29	11.8 / 0.29	7.38 / 0.32	6.31 / 0.36	5.97 / 0.39	3.66 / 0.54	3.55 / 0.55	3.58 / 0.57
	Ours	<b>4.41 / 0.43</b>	<b>3.69 / 0.51</b>	<b>3.48 / 0.55</b>	<b>3.41 / 0.57</b>	<b>3.41 / 0.58</b>	<b>3.41 / 0.59</b>	<b>3.25 / 0.63</b>	<b>3.20 / 0.74</b>	<b>3.20 / 0.76</b>
13B	Local	60.0 / 0.15	139 / 0.12	56.3 / 0.21	16.1 / 0.27	13.2 / 0.31	7.06 / 0.37	3.72 / 0.48	3.72 / 0.52	3.25 / 0.55
	H <sub>2</sub> O	12.4 / 0.39	10.4 / 0.39	8.50 / 0.40	4.56 / 0.46	3.78 / 0.49	3.58 / 0.49	3.16 / 0.55	3.28 / 0.57	3.06 / 0.59
	Elastic	14.9 / 0.30	5.75 / 0.35	4.41 / 0.40	3.55 / 0.50	3.36 / 0.52	3.28 / 0.53	2.97 / 0.58	2.89 / 0.60	3.02 / 0.59
	Ours	<b>3.72 / 0.48</b>	<b>3.17 / 0.53</b>	<b>2.97 / 0.59</b>	<b>2.92 / 0.60</b>	<b>2.89 / 0.60</b>	<b>2.84 / 0.61</b>	<b>2.77 / 0.69</b>	<b>2.73 / 0.74</b>	<b>2.73 / 0.79</b>

Table 2. Comparison with SOTA methods on MM-Vet with the PPL / ROUGE metrics under various compression ratio budgets. The results without the KV compression are 5.28 / 0.58 for LLaVA-1.5-7B and 4.72 / 0.58 for LLaVA-1.5-13B, respectively.

Model	Method	10%	20%	30%	40%	50%	60%	70%	80%	90%
7B	Local	109 / 0.11	90.0 / 0.08	99.0 / 0.13	99.0 / 0.16	66.0 / 0.16	28.4 / 0.27	12.4 / 0.34	7.88 / 0.41	6.28 / 0.46
	H <sub>2</sub> O	158 / 0.25	120 / 0.26	72.5 / 0.29	35.3 / 0.31	18.6 / 0.30	10.3 / 0.39	7.09 / 0.44	6.22 / 0.46	5.72 / 0.49
	Elastic	40.5 / 0.25	21.0 / 0.25	14.9 / 0.29	11.3 / 0.29	9.06 / 0.32	7.63 / 0.38	5.97 / 0.46	5.56 / 0.48	5.53 / 0.54
	Ours	<b>7.38 / 0.39</b>	<b>5.97 / 0.41</b>	<b>5.72 / 0.46</b>	<b>5.53 / 0.46</b>	<b>5.50 / 0.48</b>	<b>5.44 / 0.50</b>	<b>5.38 / 0.59</b>	<b>5.28 / 0.74</b>	<b>5.28 / 0.77</b>
13B	Local	135 / 0.15	120 / 0.14	77.0 / 0.24	53.8 / 0.26	40.5 / 0.27	18.0 / 0.34	9.06 / 0.42	6.63 / 0.39	5.41 / 0.43
	H <sub>2</sub> O	31.6 / 0.36	30.6 / 0.38	20.8 / 0.40	10.6 / 0.43	7.75 / 0.39	6.28 / 0.44	5.63 / 0.46	5.25 / 0.47	4.88 / 0.56
	Elastic	34.3 / 0.28	11.6 / 0.34	8.00 / 0.37	6.31 / 0.44	5.81 / 0.44	5.44 / 0.49	4.97 / 0.52	4.81 / 0.51	4.81 / 0.56
	Ours	<b>6.28 / 0.40</b>	<b>5.16 / 0.46</b>	<b>4.88 / 0.52</b>	<b>4.78 / 0.52</b>	<b>4.72 / 0.55</b>	<b>4.72 / 0.57</b>	<b>4.72 / 0.64</b>	<b>4.69 / 0.75</b>	<b>4.72 / 0.79</b>

Table 3. Global prefix configuration. Uncompressed result is 5.28.

Method	10%	20%	30%	40%	50%	60%	70%	80%	90%
Baseline	41.8	26.6	20.4	15.4	11.8	9.06	6.47	5.75	5.72
Pyramid.	20.8	10.4	7.50	5.75	5.63	5.50	5.41	<b>5.28</b>	<b>5.28</b>
PrefixKV	<b>7.38</b>	<b>5.97</b>	<b>5.72</b>	<b>5.53</b>	<b>5.50</b>	<b>5.44</b>	<b>5.38</b>	<b>5.28</b>	<b>5.28</b>

### 4.3. Model Analyses

We present comprehensive analyses for our method. Following [39], experiments are conducted on MM-Vet based on LLaVA-1.5-7B with PPL for evaluation, by default, .

**Global prefix configuration matters.** We verify the effectiveness of our method in identifying the ideal global prefix configuration. We first introduce the baseline, which keeps the same retained KV cache size for all layers. As shown in Table 3, our PrefixKV consistently brings performance benefit under various compression budgets. For example, under the compression budget of 30%, it surpasses the baseline by significant margin of 14.7 PPL. Besides, as the compression budget gradually decreases from 90% to 10%, its superiority becomes increasingly evident, showing increasing performance improvements. We also compare ours with PyramidKV [73], which manually allocates larger cache size in shallow layers and smaller size in deep layers. Since it compresses the cache only after the pre-

filling, we integrate it in the baseline for fair comparisons. As shown in Table 3, our strategy achieves superior performance over PyramidKV in various scenarios, especially under the low compression budget. These results show that compared with the same cache size across layers and the manually designed scheme by PyramidKV, our method can identify better global prefix configuration, which retains the overall contextual information more effectively.

**Inference efficiency.** We evaluate the inference efficiency of the model with our KV compression method to verify its benefit for acceleration. We follow [39] to conduct the evaluation in two practical scenarios. Specifically, firstly, we construct the input with 1024 prompt tokens and generate 512 tokens. Secondly, we employ a shorter input with 624 prompt tokens and generate 256 tokens, which means the minimal prompt length with only the image tokens and system prompts. We measure the inference time on the NVIDIA A100 GPU and use the batch size which maximizes the available memory to simulate the realistic deployment scenarios for better efficiency and throughput. As shown in Table 4, our method shows the notable inference speedups under various compression budgets compared with original model with full KV cache. For example, under the compression budget of 20% with the batch size of 16 for LLaVA-1.5-7B, our method demonstrates 1.8× inference speedup in terms of throughput. Besides, it also

Table 4. Inference time for our method under compression ratio budgets of 20% / 40% / 60% / 80%. OOM indicates out of memory.

Batch	Model	Token	Latency (s)			Throughput (token/s)	
			Size	Size	Length	PrefixKV	Full Cache
8	13B	1024+512	20.0	24.3	27.5 / 29.7	30.5	204.6 / 168.1 / 148.7 / 137.6
16	13B	624+256	11.7	14.2	15.9 / 17.3	17.8	349.5 / 288.0 / 256.3 / 236.5
16	7B	1024+512	16.8	22.5	26.6 / 29.5	30.7	486.7 / 363.3 / 307.9 / 276.9
48	7B	624+256	13.1	OOM	OOM / OOM	OOM	934.4 / OOM / OOM / OOM

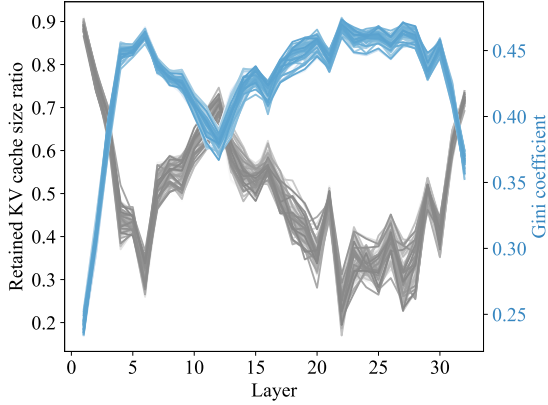


Figure 4. The retained KV cache size ratios for each layer of 100 random samples under the compression ratio of 50% and their gini coefficients of the priority sequences for KV vectors in each layer. It shows that different samples exhibit similar and robust characteristics, showing the reasonableness of offline estimation.

Table 5. Comparisons between offline estimation and online binary searching for each sample. Uncompressed result is 5.28.

Method	10%	20%	30%	40%	50%	60%	70%	80%	90%
Offline	7.38	5.97	5.72	5.53	5.50	5.44	5.38	5.28	5.28
Online	7.38	5.97	5.66	5.53	5.50	5.41	5.38	5.28	5.28

Table 6. Impact of sample numbers. Uncompressed result is 5.28.

Number	10%	20%	30%	40%	50%	60%	70%	80%	90%
1	7.63	6.03	5.72	5.53	5.53	5.44	5.38	5.28	5.28
5	7.50	6.03	5.72	5.53	5.50	5.41	5.38	5.28	5.28
10	7.38	5.97	5.72	5.53	5.50	5.44	5.38	5.28	5.28
20	7.38	5.97	5.72	5.53	5.50	5.41	5.38	5.28	5.28

reduces the memory usage, avoiding OOM and enabling efficient inference with large batch size of 48. We also note that in this scenario, our method maintains the superior performance with only 0.69 PPL decline compared with the original model. These results well demonstrate the benefit of our method in practical deployment for efficient LVLMs.

**Effect of offline estimation.** Given a compression budget, we estimate the optimal KV cache size for each layer by random samples offline, which avoids the overhead of

Table 7. Eviction or merging. Uncompressed result is 5.28.

Method	10%	20%	30%	40%	50%	60%	70%	80%	90%
PrefixKV	7.38	5.97	5.72	5.53	5.50	5.44	5.38	5.28	5.28
Position	7.63	6.06	5.75	5.53	5.44	5.31	5.31	5.28	5.28
Feature	7.38	5.97	5.72	5.53	5.44	5.31	5.28	5.28	5.28

online searching. To verify its effectiveness, we first examine the variation of retained KV cache size ratios at each layer across different samples. As shown in Figure 4, different samples exhibit the similar cache size ratios for each layer. This indicates the potential of using the samples to estimate the optimal cache size ratios offline. We further present the comparison results between offline estimation and online binary searching for each sample in Table 5. It can be observed that offline estimation can obtain the comparable performance with the online searching. Therefore, our method can be integrated into the models efficiently, without the extra inference overhead. We also inspect the impact of adopting different numbers of random samples. As shown in Table 6, the performance is stable and robust across different sample sizes. Besides, employing a single sample can achieve good performance, which shows the effectiveness of offline estimation.

**Relation between KV cache size and importance distribution.** We derive better KV cache size for each layer based on the importance distribution. To provide deeper insights for their relation, we visualize the KV cache size ratios and the gini coefficients of priority sequence for different samples in Figure 4. We observe that layers with higher gini coefficients, *i.e.*, with more concentrated importance distributions typically have fewer KV cache sizes, and vice versa. This qualitatively validates the reliability of our method, as layers with concentrated importance distributions can retain most information with fewer KV vectors, while layers with more dispersed importance distributions require larger KV cache sizes. Besides, we note that the retained KV cache size exhibits a W-shaped trend across layers. This inspires that utilizing more cost-effective attention mechanism in shallow to mid layers, as well as in mid to deep layers, may lead to more efficient model architecture.

**Eviction or merging.** Our PrefixKV shows favorable performance by cache eviction, *i.e.*, retaining the prefix vec-

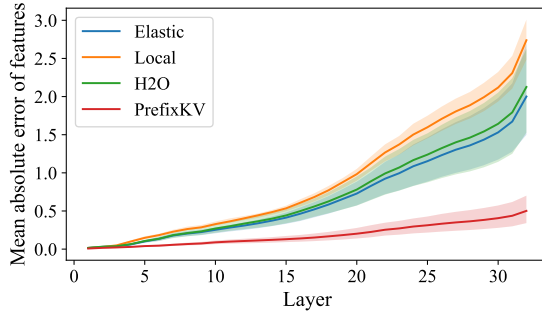


Figure 5. Mean absolute error between features of output tokens with and without compression across layers for 100 random samples. PrefixKV shows notably less feature disturbance than others.

tors and pruning the unimportant ones. To mitigate the information loss of eviction, previous research explores merging the less important KV vector with its nearest important one in position [39]. Therefore, we inspect the performance variation under combining our PrefixKV with cache merging. In addition to merging based on positional distance, we also examine the way based on the feature similarity, which are explored in the token merging field [5, 58]. Specifically, we denote the  $l$ -th layer’s retained KV vector set as  $\Omega_l^r$  and pruned set as  $\Omega_l^p$ , respectively. The cache merging operation is the same for key and value vectors in different heads, we thus proceed with the key vector for illustration and omit the head superscript. For each pruned key vector  $\mathbf{k}_l^m$  where  $m \in \Omega_l^p$ , we obtain its matching metric  $c_l^{mn}$  to each retained one  $\mathbf{k}_l^n$  where  $n \in \Omega_l^r$ . For each  $\mathbf{k}_l^n$ , we obtain the set of pruned vectors that match with it by  $\mathbf{T}_l^n = \{m \in \Omega_l^p | n = \text{argmax}_u(c_l^{mu})\}$ . The vectors are then merged to update  $\mathbf{k}_l^n$  by  $\mathbf{k}_l^{n*} = \text{Average}(\{\mathbf{k}_l^u | u \in \mathbf{T}_l^n \cup \{n\}\})$ . We experiment with matching metrics based on the positional distance and feature cosine similarity by  $c_l^{mn} = -|m - n|$  and  $c_l^{mn} = \frac{\mathbf{k}_l^m \cdot \mathbf{k}_l^n}{\|\mathbf{k}_l^m\| \|\mathbf{k}_l^n\|}$ , which are denoted as “Position” and “Feature”, respectively. As shown in Table 7, integrating “Position” can lead to inferior performance over PrefixKV in certain scenarios. We note that our method enables the maximal preservation of important KV vectors, and merging based on the positional distance, however, could introduce the interference to important cache due to the feature discrepancies among the vectors [58]. Besides, we observe that with less feature dispersion, combining “Feature” can bring the marginal improvements. This indicates that our method can well retain the significant contextual information across layers and eliminate the need for cache merging to reduce information loss, demonstrating its efficacy.

**Analyses for the feature disturbance.** To further verify the effectiveness of our method in preserving valuable contextual information across layers, we inspect the feature perturbation caused by KV cache compression for output tokens at each layer. Specifically, for each output token, we calculate the mean absolute error between its feature

Table 8. Comparisons on Qwen-VL. Uncompressed result is 6.28.

Method	10%	20%	30%	40%	50%	60%	70%	80%	90%
Local	314	185	93.0	54.5	70.0	43.8	24.6	17.5	11.4
H2O	72.5	58.0	43.3	29.3	19.1	15.4	12.9	11.1	9.50
Elastic	404	66.0	33.8	20.4	12.8	10.4	8.63	8.63	8.63
Ours	<b>16.6</b>	<b>9.94</b>	<b>8.50</b>	<b>8.13</b>	<b>7.88</b>	<b>7.09</b>	<b>6.41</b>	<b>6.28</b>	<b>6.28</b>

Table 9. Chat generation example. It shows that others fail to generate reasonable responses while ours can ensure the generation quality with better contextual information retention across layers.

	User	What do you think is going on in this snapshot?
	Local	The two girls, two girls, two girls, two girls, two girls,...
	H2O	The image shows two young girls are two young girls are two young girls are two girls...
	Elastic	The image shows a young girls are two young girls are playing with a dog is a small children are playing with a small children are two young girls are playing with a toy dog.
	Ours	The image features two young girls standing next to each other, both holding stuffed animals. One girl is holding a teddy bear, while the other girl has a stuffed dog. They appear to be enjoying their time together.

with and without compression. We employ the compression budget of 50% and visual the average error across output tokens for samples. As shown in Figure 5, our method consistently exhibits lower mean absolute error between features compared with others. This shows that our method can introduce less interference to the features of output tokens, demonstrating enhanced retention of contextual information and resulting in improved generation quality.

**Generalizability on other LVLMs.** Following [39], we conduct experiments on Qwen-VL [2] to verify the general effectiveness of our method. In Table 8, our method consistently exhibits superior performance over others across various compression budgets, highlighting its generalizability.

**Visualization of chat generation.** In Table 9, we provide the generation example in real-word scenario. We set the compression budget to 20% and observe that previous methods all fail to answer the question, generating repetitive or confusing responses. In contrast, our method delivers coherent and rational outputs, demonstrating the superiority. More examples can be referred to the supplementary.

## 5. Conclusion

In this paper, we present PrefixKV to effectively compress KV cache for efficient generation of large vision-language models (LVLMs). It derives the optimal KV cache size for

each layer by searching for the ideal global prefix configuration with the priority sequences of KV. Maximal preservation of contextual information is thus ensured layer-wisely, contributing to high-quality model generation. Extensive experiments show that our method achieves the state-of-the-art performance compared with others. It provides notable inference speedups while maintaining the generation capability, showing the superiority for practical applications.

## References

- [1] Josh Achiam, Steven Adler, Sandhini Agarwal, Lama Ahmad, Ilge Akkaya, Florencia Leoni Aleman, Diogo Almeida, Janko Altenschmidt, Sam Altman, Shyamal Anadkat, et al. Gpt-4 technical report. *arXiv preprint arXiv:2303.08774*, 2023. [1](#) [2](#)
- [2] Jinze Bai, Shuai Bai, Yunfei Chu, Zeyu Cui, Kai Dang, Xiaodong Deng, Yang Fan, Wenbin Ge, Yu Han, Fei Huang, et al. Qwen technical report. *arXiv preprint arXiv:2309.16609*, 2023. [1](#) [2](#) [8](#)
- [3] Jinze Bai, Shuai Bai, Yunfei Chu, Zeyu Cui, Kai Dang, Xiaodong Deng, Yang Fan, Wenbin Ge, Yu Han, Fei Huang, et al. Qwen technical report. *arXiv preprint arXiv:2309.16609*, 2023. [1](#)
- [4] Lucas Beyer, Andreas Steiner, André Susano Pinto, Alexander Kolesnikov, Xiao Wang, Daniel Salz, Maxim Neumann, Ibrahim Alabdulmohsin, Michael Tschannen, Emanuele Bugliarello, et al. Paligemma: A versatile 3b vlm for transfer. *arXiv preprint arXiv:2407.07726*, 2024. [2](#)
- [5] Daniel Bolya, Cheng-Yang Fu, Xiaoliang Dai, Peizhao Zhang, Christoph Feichtenhofer, and Judy Hoffman. Token merging: Your vit but faster. *arXiv preprint arXiv:2210.09461*, 2022. [8](#)
- [6] Mu Cai, Haotian Liu, Siva Karthik Mustikovela, Gregory P Meyer, Yuning Chai, Dennis Park, and Yong Jae Lee. Making large multimodal models understand arbitrary visual prompts. *arXiv preprint arXiv:2312.00784*, 2023. [2](#)
- [7] Yunkang Cao, Xiaohao Xu, Chen Sun, Xiaonan Huang, and Weiming Shen. Towards generic anomaly detection and understanding: Large-scale visual-linguistic model (gpt-4v) takes the lead. *arXiv preprint arXiv:2311.02782*, 2023. [2](#)
- [8] Hui Chen, Guiguang Ding, Zijia Lin, Sicheng Zhao, and Jun-gong Han. Show, observe and tell: Attribute-driven attention model for image captioning. In *IJCAI*, pages 606–612, 2018. [2](#)
- [9] Hui Chen, Guiguang Ding, Xudong Liu, Zijia Lin, Ji Liu, and Jungong Han. Imram: Iterative matching with recurrent attention memory for cross-modal image-text retrieval. In *Proceedings of the IEEE/CVF conference on computer vision and pattern recognition*, pages 12655–12663, 2020.
- [10] Jun Chen, Deyao Zhu, Xiaoqian Shen, Xiang Li, Zechun Liu, Pengchuan Zhang, Raghuraman Krishnamoorthi, Vikas Chandra, Yunyang Xiong, and Mohamed Elhoseiny. Minigpt-v2: large language model as a unified interface for vision-language multi-task learning. *arXiv preprint arXiv:2310.09478*, 2023. [2](#)
- [11] Keqin Chen, Zhao Zhang, Weili Zeng, Richong Zhang, Feng Zhu, and Rui Zhao. Shikra: Unleashing multi-modal llm’s referential dialogue magic. *arXiv preprint arXiv:2306.15195*, 2023. [1](#) [2](#)
- [12] Jang Hyun Cho, Boris Ivanovic, Yulong Cao, Edward Schmerling, Yue Wang, Xinshuo Weng, Boyi Li, Yurong You, Philipp Krähenbühl, Yan Wang, et al. Language-image models with 3d understanding. *arXiv preprint arXiv:2405.03685*, 2024. [2](#)
- [13] Xiangxiang Chu, Limeng Qiao, Xinyang Lin, Shuang Xu, Yang Yang, Yiming Hu, Fei Wei, Xinyu Zhang, Bo Zhang, Xiaolin Wei, et al. Mobilevlm: A fast, reproducible and strong vision language assistant for mobile devices. *arXiv preprint arXiv:2312.16886*, 2023. [2](#)
- [14] Can Cui, Yunsheng Ma, Xu Cao, Wenqian Ye, Yang Zhou, Kaizhao Liang, Jintai Chen, Juanwu Lu, Zichong Yang, Kuei-Da Liao, et al. A survey on multimodal large language models for autonomous driving. In *Proceedings of the IEEE/CVF Winter Conference on Applications of Computer Vision*, pages 958–979, 2024. [1](#) [2](#)
- [15] Wenliang Dai, Junnan Li, Dongxu Li, Anthony Meng Huat Tiong, Junqi Zhao, Weisheng Wang, Boyang Li, Pascale Fung, and Steven Hoi. Instructblip: Towards general-purpose vision-language models with instruction tuning, 2023. [1](#) [2](#)
- [16] Zixuan Ding, Ao Wang, Hui Chen, Qiang Zhang, Pengzhang Liu, Yongjun Bao, Weipeng Yan, and Jungong Han. Exploring structured semantic prior for multi label recognition with incomplete labels. In *Proceedings of the IEEE/CVF Conference on Computer Vision and Pattern Recognition*, pages 3398–3407, 2023. [2](#)
- [17] Robert Dorfman. A formula for the gini coefficient. *The review of economics and statistics*, pages 146–149, 1979. [4](#)
- [18] Abhimanyu Dubey, Abhinav Jauhri, Abhinav Pandey, Abhishek Kadian, Ahmad Al-Dahle, Aiesha Letman, Akhil Mathur, Alan Schelten, Amy Yang, Angela Fan, et al. The llama 3 herd of models. *arXiv preprint arXiv:2407.21783*, 2024. [1](#) [2](#)
- [19] Joseph L Gastwirth. A general definition of the lorenz curve. *Econometrica: Journal of the Econometric Society*, pages 1037–1039, 1971. [4](#)
- [20] Joseph L Gastwirth. The estimation of the lorenz curve and gini index. *The review of economics and statistics*, pages 306–316, 1972. [4](#)
- [21] Yuxian Gu, Li Dong, Furu Wei, and Minlie Huang. Minillm: Knowledge distillation of large language models. In *The Twelfth International Conference on Learning Representations*, 2024. [2](#)
- [22] Zhaopeng Gu, Bingke Zhu, Guibo Zhu, Yingying Chen, Ming Tang, and Jinqiao Wang. Anomalygpt: Detecting industrial anomalies using large vision-language models. In *Proceedings of the AAAI Conference on Artificial Intelligence*, pages 1932–1940, 2024. [2](#)
- [23] Yining Hong, Haoyu Zhen, Peihao Chen, Shuhong Zheng, Yilun Du, Zhenfang Chen, and Chuang Gan. 3d-llm: Injecting the 3d world into large language models. *Advances in Neural Information Processing Systems*, 36:20482–20494, 2023. [2](#)

[24] Andrew G Howard. Mobilenets: Efficient convolutional neural networks for mobile vision applications. *arXiv preprint arXiv:1704.04861*, 2017. 2

[25] Cheng-Yu Hsieh, Chun-Liang Li, Chih-Kuan Yeh, Hootan Nakhost, Yasuhisa Fujii, Alexander Ratner, Ranjay Krishna, Chen-Yu Lee, and Tomas Pfister. Distilling step-by-step! outperforming larger language models with less training data and smaller model sizes. *arXiv preprint arXiv:2305.02301*, 2023. 2

[26] IDEFICS. Introducing idefics: An open reproduction of state-of-the-art visual language model. <https://huggingface.co/blog/idefics>, 2023. 1

[27] Andrew Jaegle, Felix Gimeno, Andy Brock, Oriol Vinyals, Andrew Zisserman, and Joao Carreira. Perceiver: General perception with iterative attention. In *International conference on machine learning*, pages 4651–4664. PMLR, 2021. 2

[28] Albert Q Jiang, Alexandre Sablayrolles, Arthur Mensch, Chris Bamford, Devendra Singh Chaplot, Diego de las Casas, Florian Bressand, Gianna Lengyel, Guillaume Lampe, Lucile Saulnier, et al. Mistral 7b. *arXiv preprint arXiv:2310.06825*, 2023. 1, 2

[29] Chunyuan Li, Cliff Wong, Sheng Zhang, Naoto Usuyama, Haotian Liu, Jianwei Yang, Tristan Naumann, Hoifung Poon, and Jianfeng Gao. Llava-med: Training a large language-and-vision assistant for biomedicine in one day. *Advances in Neural Information Processing Systems*, 36, 2024. 1, 2

[30] Feng Li, Renrui Zhang, Hao Zhang, Yuanhan Zhang, Bo Li, Wei Li, Zejun Ma, and Chunyuan Li. Llava-next-interleave: Tackling multi-image, video, and 3d in large multimodal models. *arXiv preprint arXiv:2407.07895*, 2024. 2

[31] Yanwei Li, Yuechen Zhang, Chengyao Wang, Zhisheng Zhong, Yixin Chen, Ruihang Chu, Shaoteng Liu, and Jiaya Jia. Mini-gemini: Mining the potential of multi-modality vision language models. *arXiv preprint arXiv:2403.18814*, 2024. 2

[32] Zeju Li, Chao Zhang, Xiaoyan Wang, Rui long Ren, Yifan Xu, Ruifei Ma, Xiangde Liu, and Rong Wei. 3dmit: 3d multi-modal instruction tuning for scene understanding. In *2024 IEEE International Conference on Multimedia and Expo Workshops (ICMEW)*, pages 1–5. IEEE, 2024. 2

[33] Bin Lin, Bin Zhu, Yang Ye, Munan Ning, Peng Jin, and Li Yuan. Video-llava: Learning united visual representation by alignment before projection. *arXiv preprint arXiv:2311.10122*, 2023. 2

[34] Chin-Yew Lin. Rouge: A package for automatic evaluation of summaries. In *Text summarization branches out*, pages 74–81, 2004. 5

[35] Ji Lin, Jiaming Tang, Haotian Tang, Shang Yang, Wei-Ming Chen, Wei-Chen Wang, Guangxuan Xiao, Xingyu Dang, Chuang Gan, and Song Han. Awq: Activation-aware weight quantization for on-device llm compression and acceleration. *Proceedings of Machine Learning and Systems*, 6:87–100, 2024. 2

[36] Haotian Liu, Chunyuan Li, Yuheng Li, and Yong Jae Lee. Improved baselines with visual instruction tuning. In *Proceedings of the IEEE/CVF Conference on Computer Vision and Pattern Recognition*, pages 26296–26306, 2024. 1, 2, 5

[37] Haotian Liu, Chunyuan Li, Qingyang Wu, and Yong Jae Lee. Visual instruction tuning. *Advances in neural information processing systems*, 36, 2024. 1, 2

[38] Zechun Liu, Barlas Onguz, Changsheng Zhao, Ernie Chang, Pierre Stock, Yashar Mehdad, Yangyang Shi, Raghuraman Krishnamoorthi, and Vikas Chandra. Llm-qat: Data-free quantization aware training for large language models. *arXiv preprint arXiv:2305.17888*, 2023. 2

[39] Zuyan Liu, Benlin Liu, Jiahui Wang, Yuhao Dong, Guangyi Chen, Yongming Rao, Ranjay Krishna, and Jiwen Lu. Efficient inference of vision instruction-following models with elastic cache. *arXiv preprint arXiv:2407.18121*, 2024. 1, 2, 3, 4, 5, 6, 8

[40] Xinyin Ma, Gongfan Fang, and Xinchao Wang. Llm-pruner: On the structural pruning of large language models. *Advances in neural information processing systems*, 36:21702–21720, 2023. 2

[41] Zhiliang Peng, Wenhui Wang, Li Dong, Yaru Hao, Shaohan Huang, Shuming Ma, and Furu Wei. Kosmos-2: Grounding multimodal large language models to the world. *arXiv preprint arXiv:2306.14824*, 2023. 2

[42] Reiner Pope, Sholto Douglas, Aakanksha Chowdhery, Jacob Devlin, James Bradbury, Jonathan Heek, Kefan Xiao, Shivanai Agrawal, and Jeff Dean. Efficiently scaling transformer inference. *Proceedings of Machine Learning and Systems*, 5: 606–624, 2023. 1, 3

[43] Fangxun Shu, Yue Liao, Le Zhuo, Chenning Xu, Guanghao Zhang, Haonan Shi, Long Chen, Tao Zhong, Wanggui He, Siming Fu, et al. Llava-mod: Making llava tiny via moe knowledge distillation. *arXiv preprint arXiv:2408.15881*, 2024. 2

[44] Sharath Turuvekere Sreenivas, Saurav Muralidharan, Raviraj Joshi, Marcin Chochowski, Mostafa Patwary, Mohammad Shoeybi, Bryan Catanzaro, Jan Kautz, and Pavlo Molchanov. Llm pruning and distillation in practice: The minitron approach. *arXiv preprint arXiv:2408.11796*, 2024. 2

[45] Mingjie Sun, Zhuang Liu, Anna Bair, and J Zico Kolter. A simple and effective pruning approach for large language models. *arXiv preprint arXiv:2306.11695*, 2023. 2

[46] Gemini Team, Rohan Anil, Sebastian Borgeaud, Jean-Baptiste Alayrac, Jiahui Yu, Radu Soricut, Johan Schalkwyk, Andrew M Dai, Anja Hauth, Katie Millican, et al. Gemini: a family of highly capable multimodal models. *arXiv preprint arXiv:2312.11805*, 2023. 1, 2

[47] Gemma Team, Thomas Mesnard, Cassidy Hardin, Robert Dadashi, Surya Bhupatiraju, Shreya Pathak, Laurent Sifre, Morgane Rivière, Mihir Sanjay Kale, Juliette Love, et al. Gemma: Open models based on gemini research and technology. *arXiv preprint arXiv:2403.08295*, 2024.

[48] Gemma Team, Morgane Rivière, Shreya Pathak, Pier Giuseppe Sessa, Cassidy Hardin, Surya Bhupatiraju, Léonard Hussenot, Thomas Mesnard, Bobak Shahriari, Alexandre Ramé, et al. Gemma 2: Improving open language models at a practical size. *arXiv preprint arXiv:2408.00118*, 2024. 2

[49] Xiaoyu Tian, Junru Gu, Bailin Li, Yicheng Liu, Yang Wang, Zhiyong Zhao, Kun Zhan, Peng Jia, Xianpeng Lang, and

Hang Zhao. Drivevlm: The convergence of autonomous driving and large vision-language models. *arXiv preprint arXiv:2402.12289*, 2024. 2

[50] Hugo Touvron, Thibaut Lavril, Gautier Izacard, Xavier Martinet, Marie-Anne Lachaux, Timothée Lacroix, Baptiste Rozière, Naman Goyal, Eric Hambro, Faisal Azhar, et al. Llama: Open and efficient foundation language models. *arXiv preprint arXiv:2302.13971*, 2023. 1, 2

[51] Hugo Touvron, Louis Martin, Kevin Stone, Peter Albert, Amjad Almahairi, Yasmine Babaei, Nikolay Bashlykov, Soumya Batra, Prajwal Bhargava, Shruti Bhosale, et al. Llama 2: Open foundation and fine-tuned chat models. *arXiv preprint arXiv:2307.09288*, 2023. 1, 2

[52] Minh-Hao Van, Prateek Verma, and Xintao Wu. On large visual language models for medical imaging analysis: An empirical study. In *2024 IEEE/ACM Conference on Connected Health: Applications, Systems and Engineering Technologies (CHASE)*, pages 172–176. IEEE, 2024. 1, 2

[53] Ao Wang, Hui Chen, Zijia Lin, Zixuan Ding, Pengzhang Liu, Yongjun Bao, Weipeng Yan, and Guiguang Ding. Hierarchical prompt learning using clip for multi-label classification with single positive labels. In *Proceedings of the 31st ACM International Conference on Multimedia*, pages 5594–5604, 2023. 2

[54] Ao Wang, Hui Chen, Zijia Lin, Sicheng Zhao, Jungong Han, and Guiguang Ding. Cait: Triple-win compression towards high accuracy, fast inference, and favorable transferability for vits. *arXiv preprint arXiv:2309.15755*, 2023. 2

[55] Ao Wang, Hui Chen, Zijia Lin, Jungong Han, and Guiguang Ding. Repvit: Revisiting mobile cnn from vit perspective. In *Proceedings of the IEEE/CVF Conference on Computer Vision and Pattern Recognition*, pages 15909–15920, 2024.

[56] Ao Wang, Hui Chen, Lihao Liu, Kai Chen, Zijia Lin, Jungong Han, and Guiguang Ding. Yolov10: Real-time end-to-end object detection. *arXiv preprint arXiv:2405.14458*, 2024. 2

[57] Wenhui Wang, Jiangwei Xie, ChuanYang Hu, Haoming Zou, Jianan Fan, Wenwen Tong, Yang Wen, Silei Wu, Hanming Deng, Zhiqi Li, et al. Drivemlm: Aligning multi-modal large language models with behavioral planning states for autonomous driving. *arXiv preprint arXiv:2312.09245*, 2023. 1

[58] Siyuan Wei, Tianzhu Ye, Shen Zhang, Yao Tang, and Jianjun Liang. Joint token pruning and squeezing towards more aggressive compression of vision transformers. In *Proceedings of the IEEE/CVF Conference on Computer Vision and Pattern Recognition*, pages 2092–2101, 2023. 8

[59] Jiaxiang Wu, Cong Leng, Yuhang Wang, Qinghao Hu, and Jian Cheng. Quantized convolutional neural networks for mobile devices. In *Proceedings of the IEEE conference on computer vision and pattern recognition*, pages 4820–4828, 2016. 2

[60] Guangxuan Xiao, Ji Lin, Mickael Seznec, Hao Wu, Julien Demouth, and Song Han. Smoothquant: Accurate and efficient post-training quantization for large language models. In *International Conference on Machine Learning*, pages 38087–38099. PMLR, 2023. 2

[61] Guangxuan Xiao, Yuandong Tian, Beidi Chen, Song Han, and Mike Lewis. Efficient streaming language models with attention sinks. *arXiv preprint arXiv:2309.17453*, 2023. 1, 2, 3, 5

[62] Lin Xu, Yilin Zhao, Daquan Zhou, Zhijie Lin, See Kiong Ng, and Jiashi Feng. Pllava: Parameter-free llava extension from images to videos for video dense captioning. *arXiv preprint arXiv:2404.16994*, 2024. 2

[63] Aiyuan Yang, Bin Xiao, Bingning Wang, Borong Zhang, Ce Bian, Chao Yin, Chenxu Lv, Da Pan, Dian Wang, Dong Yan, et al. Baichuan 2: Open large-scale language models. *arXiv preprint arXiv:2309.10305*, 2023. 1

[64] Fan Yang, Sicheng Zhao, Yanhao Zhang, Haoxiang Chen, Hui Chen, Wenbo Tang, Haonan Lu, Pengfei Xu, Zhenyu Yang, Jungong Han, et al. Llmi3d: Empowering llm with 3d perception from a single 2d image. *arXiv preprint arXiv:2408.07422*, 2024. 2

[65] Zhengyuan Yang, Linjie Li, Kevin Lin, Jianfeng Wang, Chung-Ching Lin, Zicheng Liu, and Lijuan Wang. The dawn of lmms: Preliminary explorations with gpt-4v (ision). *arXiv preprint arXiv:2309.17421*, 9(1):1, 2023. 2

[66] Shukang Yin, Chaoyou Fu, Sirui Zhao, Ke Li, Xing Sun, Tong Xu, and Enhong Chen. A survey on multimodal large language models. *arXiv preprint arXiv:2306.13549*, 2023. 3

[67] Junwei You, Haotian Shi, Zhuoyu Jiang, Zilin Huang, Rui Gan, Keshu Wu, Xi Cheng, Xiaopeng Li, and Bin Ran. V2x-vlm: End-to-end v2x cooperative autonomous driving through large vision-language models. *arXiv preprint arXiv:2408.09251*, 2024. 2

[68] Weihao Yu, Zhengyuan Yang, Linjie Li, Jianfeng Wang, Kevin Lin, Zicheng Liu, Xinchao Wang, and Lijuan Wang. Mm-vet: Evaluating large multimodal models for integrated capabilities. *arXiv preprint arXiv:2308.02490*, 2023. 5

[69] Zhengqing Yuan, Zhaoxu Li, and Lichao Sun. Tinygpt-v: Efficient multimodal large language model via small backbones. *arXiv preprint arXiv:2312.16862*, 2023. 2

[70] Kaiyu Yue, Bor-Chun Chen, Jonas Geiping, Hengduo Li, Tom Goldstein, and Ser-Nam Lim. Object recognition as next token prediction. In *Proceedings of the IEEE/CVF Conference on Computer Vision and Pattern Recognition*, pages 16645–16656, 2024. 2

[71] Hang Zhang, Xin Li, and Lidong Bing. Video-llama: An instruction-tuned audio-visual language model for video understanding. *arXiv preprint arXiv:2306.02858*, 2023. 2

[72] Shilong Zhang, Peize Sun, Shoufa Chen, Min Xiao, Wenqi Shao, Wenwei Zhang, Yu Liu, Kai Chen, and Ping Luo. Gpt4roi: Instruction tuning large language model on region-of-interest. *arXiv preprint arXiv:2307.03601*, 2023. 1, 2

[73] Yichi Zhang, Bofei Gao, Tianyu Liu, Keming Lu, Wayne Xiong, Yue Dong, Baobao Chang, Junjie Hu, Wen Xiao, et al. Pyramidkv: Dynamic kv cache compression based on pyramidal information funneling. *arXiv preprint arXiv:2406.02069*, 2024. 6

[74] Yuhui Zhang, Alyssa Unell, Xiaohan Wang, Dhruba Ghosh, Yuchang Su, Ludwig Schmidt, and Serena Yeung-Levy. Why are visually-grounded language models bad at image classification? *arXiv preprint arXiv:2405.18415*, 2024. 2

[75] Zhenyu Zhang, Ying Sheng, Tianyi Zhou, Tianlong Chen, Lianmin Zheng, Ruiqi Cai, Zhao Song, Yuandong Tian, Christopher Ré, Clark Barrett, et al. H2o: Heavy-hitter oracle for efficient generative inference of large language models. *Advances in Neural Information Processing Systems*, 36, 2024. [1](#), [2](#), [3](#), [5](#)

[76] Wayne Xin Zhao, Kun Zhou, Junyi Li, Tianyi Tang, Xiaolei Wang, Yupeng Hou, Yingqian Min, Beichen Zhang, Junjie Zhang, Zican Dong, et al. A survey of large language models. *arXiv preprint arXiv:2303.18223*, 2023. [3](#)

[77] Baichuan Zhou, Ying Hu, Xi Weng, Junlong Jia, Jie Luo, Xien Liu, Ji Wu, and Lei Huang. Tinyllava: A framework of small-scale large multimodal models. *arXiv preprint arXiv:2402.14289*, 2024. [2](#)

[78] Zixuan Zhou, Xuefei Ning, Ke Hong, Tianyu Fu, Jiaming Xu, Shiyao Li, Yuming Lou, Luning Wang, Zhihang Yuan, Xiuhong Li, et al. A survey on efficient inference for large language models. *arXiv preprint arXiv:2404.14294*, 2024. [3](#)

[79] Deyao Zhu, Jun Chen, Xiaoqian Shen, Xiang Li, and Mohamed Elhoseiny. Minigpt-4: Enhancing vision-language understanding with advanced large language models. *arXiv preprint arXiv:2304.10592*, 2023. [2](#)

[80] Yichen Zhu, Minjie Zhu, Ning Liu, Zhicai Ou, Xiaofeng Mou, and Jian Tang. Llava-phi: Efficient multi-modal assistant with small language model, 2024. [2](#)